

Angular-momentum-gated light-particle evaporation spectra from $^{97}\text{Tc}^*$ and $^{62}\text{Zn}^*$ systems

Pratap Roy,* K. Banerjee, S. Bhattacharya, C. Bhattacharya, S. Kundu, T. K. Rana, T. K. Ghosh, G. Mukherjee, R. Pandey, J. K. Meena, M. Gohil, H. Pai, V. Srivastava, A. Dey, Deepak Pandit, S. Mukhopadhyay, S. Pal, and S. R. Banerjee

Variable Energy Cyclotron Centre, 1/AF, Bidhan Nagar, Kolkata 700 064, India

(Received 24 July 2012; revised manuscript received 11 September 2012; published 22 October 2012)

Light particle (n , p , and α) evaporation spectra have been measured in coincidence with γ rays of different multiplicities, emitted from $^{97}\text{Tc}^*$ and $^{62}\text{Zn}^*$ compound systems at the excitation energies ~ 36 MeV. Statistical model analysis of the experimental data have been carried out to extract the value of the inverse level density parameter (k) at different angular momentum regions, corresponding to different γ multiplicity. A systematic trend of a decrease of inverse level density parameter with the increase in angular momentum has been observed from the study of all three evaporation spectra, for both systems. Simultaneous analysis of all (major) light particle spectra provide useful information to understand the angular momentum dependence of nuclear level density in a consistent manner.

DOI: [10.1103/PhysRevC.86.044622](https://doi.org/10.1103/PhysRevC.86.044622)

PACS number(s): 24.60.Dr, 25.70.Gh, 24.10.Pa

I. INTRODUCTION

Study of evaporation spectra of particles emitted from an excited compound nucleus gives useful information about the nuclear level density (NLD). Knowledge of nuclear level density in turn can provide an interesting test of different microscopic approaches of nuclear structure used to calculate NLD. Apart from this fundamental interest, level densities are important ingredients for both the statistical and pre-equilibrium models of nuclear reactions. In statistical models total level densities are required, whereas pre-equilibrium models need partial level densities (involving only restricted numbers of fermions). Even after substantial theoretical efforts it is not yet possible to have a complete microscopic solution including all known nuclear effects that can lead to a complete analytical form of NLD. The understanding of the variation of NLD over a wide range of excitation energy and angular momentum comes only from the phenomenology based semiempirical formulations. One such formulation, which is widely used in statistical model calculations, is based on the Fermi gas model. For a spherical nucleus of mass number A at moderate excitation energy E^* and spin J , the nuclear level density, $\rho_{\text{int}}(E^*, J)$, as predicted by the Fermi gas model [1] is given by

$$\rho_{\text{int}}(E^*, J) = \frac{(2J+1)}{12} \left(\frac{\hbar^2}{2\mathfrak{I}_{\text{eff}}} \right)^{3/2} \sqrt{a} \times \frac{\exp(2\sqrt{a}(E^* - E_{\text{rot}} - \Delta p))}{(E^* - E_{\text{rot}} - \Delta p)^2}. \quad (1)$$

Where a is called the level density parameter. Here

$$E_{\text{rot}} = \frac{\hbar^2}{2\mathfrak{I}} J(J+1) \quad (2)$$

is the rotational energy, and

$$\mathfrak{I}_{\text{eff}} = \mathfrak{I}_0(1 + \delta_1 J^2 + \delta_2 J^4) \quad (3)$$

is the effective moment of inertia of the system [2]. Here r_0 , δ_1 and δ_2 , Δp , \mathfrak{I}_0 , and E^* are the radius parameter, deformability coefficients, pairing energy, rigid body moment of inertia, and excitation energy, respectively. The NLD parameter a is related to the density of the single particle levels near the Fermi surface and is influenced by the shell structure and the shape of the nucleus, which in turn depend on the excitation energy. An improved excitation energy dependent parametrization of the nuclear level density parameter has been proposed by Ignatyuk *et al.*, [3] which incorporated the effect of nuclear shell structure at low excitation energy and goes smoothly to the liquid drop value at higher excitation energy. This is expressed as

$$a = \tilde{a} \left[1 - \frac{\Delta S}{U} \{1 - \exp(-\gamma U)\} \right], \quad (4)$$

$$\gamma^{-1} = \frac{0.4A^{4/3}}{\tilde{a}}, \quad (5)$$

where \tilde{a} is the asymptotic value of the liquid drop NLD parameter at the excitation energy where shell effects are depleted leaving a smooth dependence on A . Here ΔS is the shell correction obtained from the difference of the experimental and the liquid drop model masses and γ is the rate at which the shell effect is depleted with the increase in excitation energy.

The spin dependence in NLD at high E^* and J is incorporated through the spin dependent rotational energy E_{rot} [2]. The quantities δ_1 and δ_2 in Eq. (3) are adjustable input parameters providing a range of choices for the spin dependence of the level density. In the present formulation of $\rho_{\text{int}}(E^*, J)$ any dependence of the level-density parameter a on spin or deformation is incorporated by E_{rot} . However, this prescription is mostly tested with the inclusive particle spectra. Exclusive measurement with respect to angular momentum may reveal additional detail on the spin dependence of NLD [4–7].

It may be noted that the level density prescription as given by Eq. (1) is based on the independent particle picture of the nucleus. However, additional contribution to NLD beyond the independent particle model may come from the collective properties (rotation and/or vibration) which involve coherent excitations of the nucleons. It can be shown that [8,9] if collective states are accounted for then the level density

*pratap_presi@yahoo.co.in

$\rho_{\text{int}}(E^*, J)$ is enhanced. In this situation total nuclear level density is given by

$$\rho(E^*, J) = \rho_{\text{int}}(E^*, J)K_{\text{coll}}(E^*), \quad (6)$$

where K_{coll} is the collective enhancement factor, which is proposed to be damped and finally vanishes ($K_{\text{coll}} \rightarrow 1$) as the temperature crosses a critical value [8].

It is important and interesting to understand the dependence of NLD on the key parameters such as excitation energy (temperature) and the angular momentum. In recent years, there have been renewed interest in understanding the angular momentum dependence of nuclear level density. In a couple of recent experiments [5,6], angular momentum dependences of NLD were studied by analyzing the α -particle evaporation spectra emitted from various compound systems. In one of these experiments with $A \sim 180$, $E^* \sim 56$ –59, and $\langle J \rangle \sim 15$ –30 \hbar , the inverse level density parameter k ($k = A/\bar{a}$) was found to remain constant within the statistical errors in the measured angular momentum range [5]. In the other experiment performed at $A \sim 120$, $E^* \sim 60$ MeV and $J \sim 10$ –20 \hbar , no systematic variation of inverse level density parameter was observed [6]. For $Z_R = 49, 50$, and 51 (Z_R is the atomic number of the evaporation residue) k was found to be constant while for the other cases it was observed to increase with increasing angular momentum. On the other hand theoretical calculations for similar systems showed that the inverse level density parameters should increase for all the cases [10]. However, in a recent measurement of angular momentum gated neutron evaporation spectra for $A \sim 118$, $E^* \sim 31$ MeV and 43 MeV and $J \sim 10$ –20 \hbar , we have shown that the inverse level density parameter decreases with increasing angular momentum. Thus, there is a relative increase of nuclear level density at higher J values, which could be a signature of the collective enhancement [4].

So, even after all these studies our understanding on the variation of NLD as a function of angular momentum is not conclusive and requires further investigations. Moreover, it would also be interesting to observe the variation of nuclear level density parameter as a function of J estimated from different light particle measurement simultaneously. Such measurement to our knowledge has not been carried out in the past. In order to extract the value of the level density parameter and to see its angular momentum dependence, we have measured the light-particle (n , p , and α) evaporation spectra along with the γ -ray multiplicity in ${}^4\text{He}$ on ${}^{93}\text{Nb}$ (${}^{97}\text{Tc}^*$) and ${}^4\text{He}$ on ${}^{58}\text{Ni}$ (${}^{62}\text{Zn}^*$) reactions. The simultaneous analysis of all light particle evaporation spectra in the same experiment may be helpful in understanding the angular momentum dependence of NLD in more consistent manner.

II. EXPERIMENTAL DETAIL

The experiments were performed using 35 MeV ${}^4\text{He}$ ion beam from the K-130 cyclotron accelerator facility at the Variable Energy Cyclotron Centre. Two self-supporting foils of ${}^{93}\text{Nb}$ and ${}^{58}\text{Ni}$ (99.9% enriched) with thicknesses ~ 1 mg/cm² were used as the targets. The compound nuclei

${}^{97}\text{Tc}^*$ (${}^4\text{He} + {}^{93}\text{Nb}$) and ${}^{62}\text{Zn}^*$ (${}^4\text{He} + {}^{58}\text{Ni}$) were populated by the complete fusion reactions at the excitation energies of 36 MeV. To detect and identify the charged particles emitted during the compound nuclear evaporation process, a three-element telescope consisting of a 50 μm single-sided silicon strip detector (16 channels), 500 μm double-sided silicon strip detector (16 \times 16 channels), and two CsI(Tl) crystals (thickness 4 cm) at the back, were mounted at the mean angle of 147° covering an angular range of 17.5°. The emitted neutrons were detected using four liquid-scintillator (BC501A) detectors of dimension 7 in. \times 5 in. [11], each covering a solid angle ~ 5.63 mSr. The neutron detectors were placed outside the scattering chamber at angles 92°, 107°, 121°, and 151° with respect to the beam direction at a distance of 150 cm from the target. To keep the background of the neutron detector at minimum level, the beam dump was kept at 3 m away from the target and was well shielded with layers of lead and borated paraffin. The energy of the emitted neutrons has been measured using the time of flight (TOF) technique whereas the neutron γ -ray discrimination was achieved by both pulse shape discrimination (PSD) and time of flight. In the present experiment, populated angular momenta were estimated by measuring the γ -ray multiplicity using a 50 element BaF₂ based low energy γ -ray filter array [12]. The

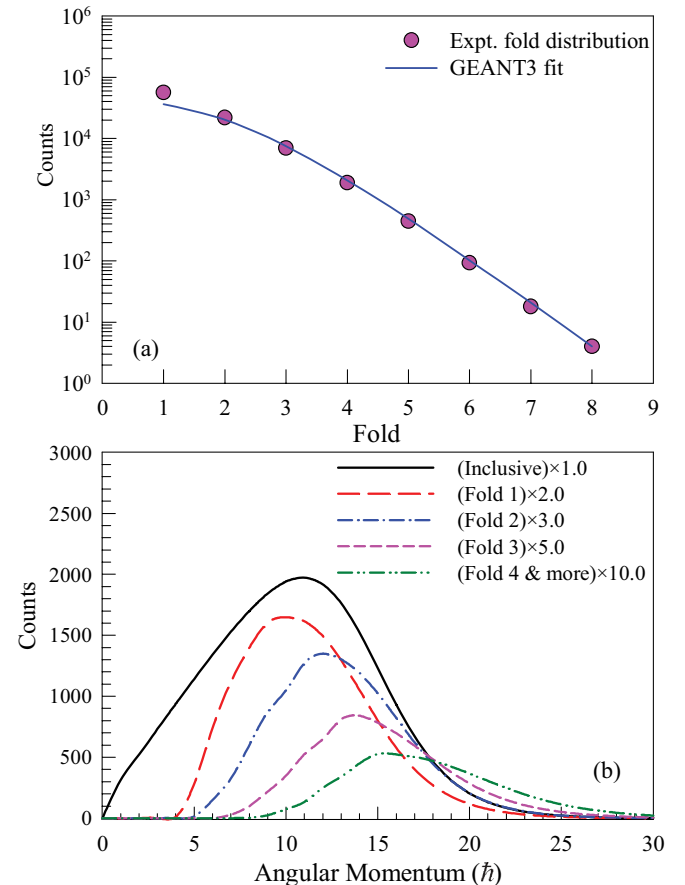


FIG. 1. (Color online) (a) Measured fold distribution along with GEANT3 simulation fit and (b) angular momentum distribution for different folds for the ${}^4\text{He} + {}^{58}\text{Ni}$ system.

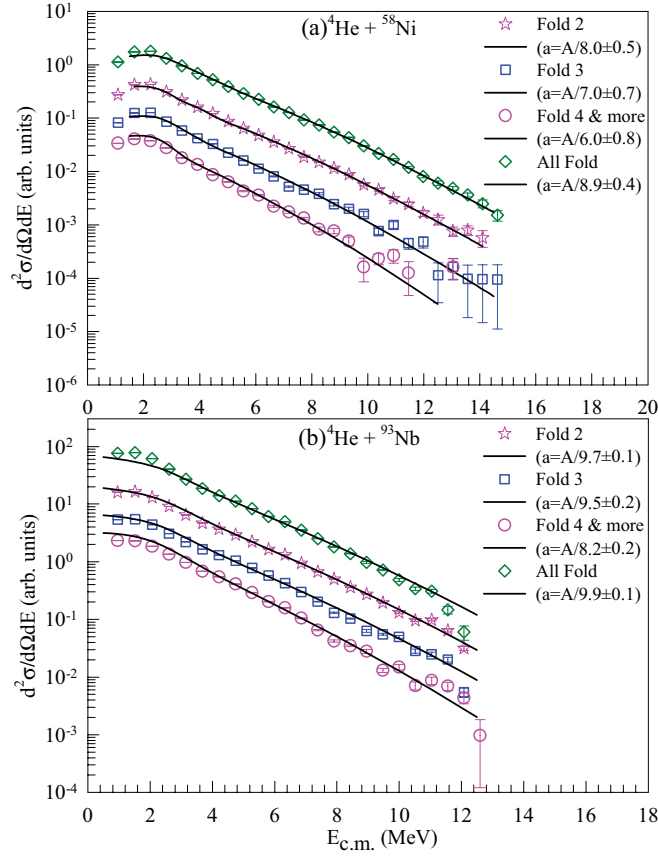


FIG. 2. (Color online) Experimental neutron spectra for different folds along with the theoretical fits (continuous lines) using statistical model code CASCADE for (a) ${}^4\text{He} + {}^{58}\text{Ni}$ and (b) ${}^4\text{He} + {}^{93}\text{Nb}$ systems.

filter was split into two blocks of 25 detectors each and were placed on the top and bottom of the thin wall reaction chamber (wall thickness ~ 3 mm) in a staggered castle type geometry. Typical solid angle coverage of the multiplicity filter was about $\sim 33\%$. Data from the neutron and the charge particle detectors were recorded in event-by-event mode in coincidence with γ fold. Here fold is defined as the number of BaF_2 detectors fired simultaneously in an event, which is directly related to the populated angular momentum. Because of the low statistics of the α -particle spectra obtained in this experiment, the α -particle measurement has been repeated in another experiment, using silicon surface barrier ΔE - E telescope in place of the three-element telescope used in the earlier measurement. The ΔE detector thickness was $50 \mu\text{m}$ for ${}^{93}\text{Nb}$ reaction, whereas a $10 \mu\text{m}$ thick detector was used for the ${}^{58}\text{Ni}$ reaction, so as to keep the detection threshold below the coulomb bump. The E detector thickness was $500 \mu\text{m}$ in both cases. Other experimental arrangements of the repeat experiment were unchanged from the previous measurement.

III. RESULTS AND DISCUSSIONS

The background corrected neutron, proton, and α -particle energy spectra measured at various laboratory angles were

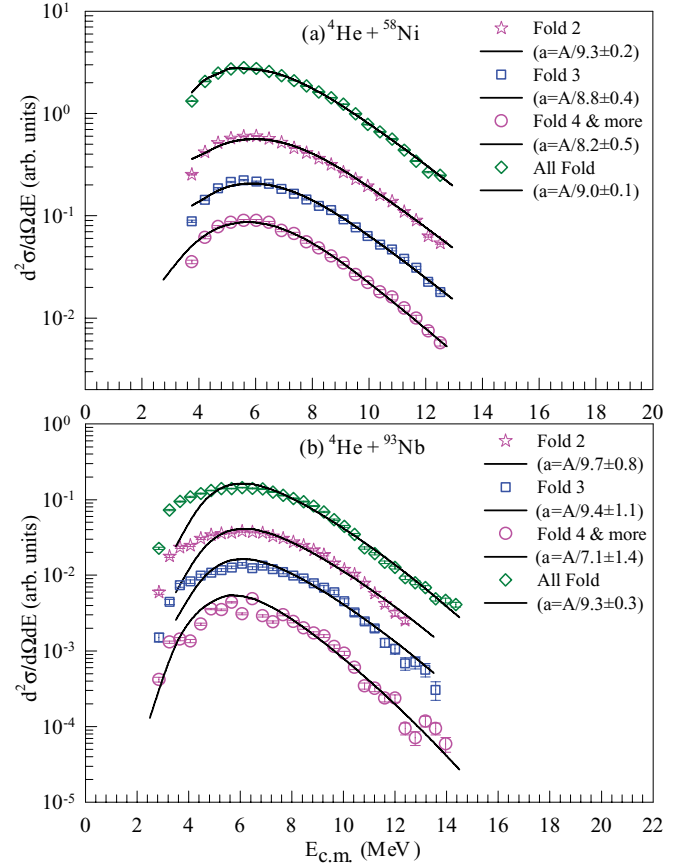


FIG. 3. (Color online) Same as Fig. 2 but for protons.

transformed to the compound nucleus center-of-mass (c.m.) system using the standard Jacobian transformation. In the center-of-mass system, the spectra measured at different back angles overlapped very well, indicating that the spectra originated from an equilibrated compound nuclear source. In converting the neutron TOF to neutron energy, the prompt γ peak in TOF spectrum was used as the time reference. The efficiency correction for the neutron detectors were performed using the Monte Carlo computer code NEFF [13]. The angular momentum distributions for different folds were obtained by converting the measured γ -fold distribution using the Monte Carlo simulation technique based on the GEANT3 toolkit [14]. The measured fold distribution for ${}^4\text{He} + {}^{58}\text{Ni}$ system has been displayed in Fig. 1(a) along with the corresponding GEANT3 simulation fit. The extracted angular momentum distributions corresponding to different folds have also been shown in Fig. 1(b). The theoretical neutron, proton, and α -particle energy spectra were calculated using the statistical model code CASCADE [15], with the extracted angular momentum distributions for different folds as input. To have a better comparison with the experimental data, the calculated CASCADE spectra for neutrons were convoluted with the TOF energy resolution of the neutron detector [4]. The experimental neutron, proton, and α -particle energy spectra (symbols) along with the CASCADE predictions (continuous lines) are shown in Figs. 3–5, respectively. In the CASCADE calculation, the phenomenological level density formula given by Eq. (1) was

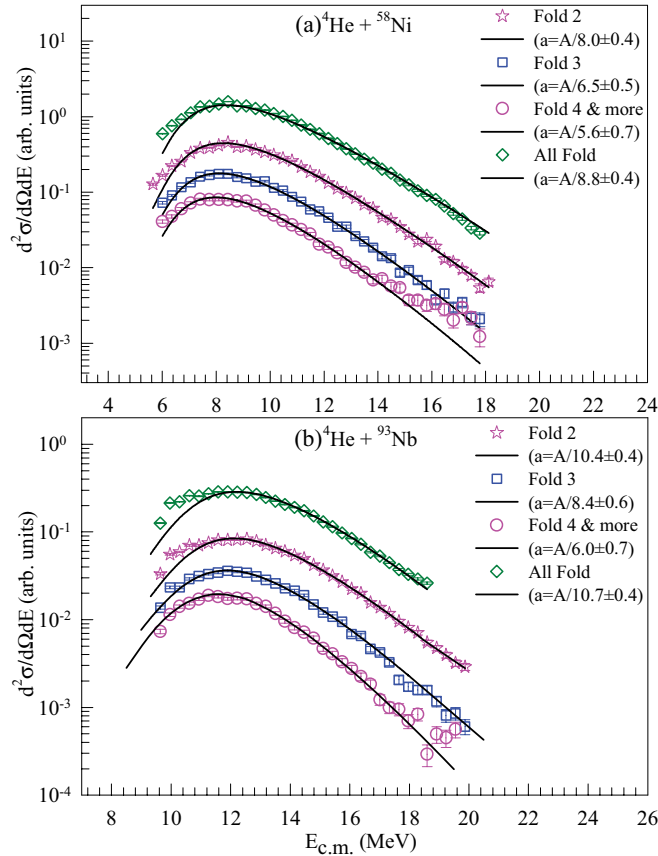


FIG. 4. (Color online) Same as Fig. 2 for α -particles.

used. The transmission coefficients were calculated using the optical model, where the optical model (OM) parameters for neutron, proton, and α -particle were taken from Refs. [16–18], respectively. The shape of the kinetic energy spectra were mostly determined by the value of the level density parameter. The role of the deformability parameters (δ_1 and δ_2) was found to be insignificant for neutron and proton spectra for both ${}^4\text{He} + {}^{58}\text{Ni}$ and ${}^4\text{He} + {}^{93}\text{Nb}$ systems. However, the shape of the α -particle spectra showed appreciable change with the variation of δ_1 and δ_2 in case of ${}^4\text{He} + {}^{58}\text{Ni}$ system, although for ${}^4\text{He} + {}^{93}\text{Nb}$ system role of δ_1 and δ_2 were still insignificant. Figure 5 shows the effect of δ_1 and δ_2 in the ‘*all fold*’ α -particle spectra for ${}^4\text{He} + {}^{58}\text{Ni}$ and ${}^4\text{He} + {}^{93}\text{Nb}$ systems. Here ‘*all fold*’ refers to the sum of all folds 1, 2, 3, and 4 & more. The shape of α -particle spectra for the ${}^4\text{He} + {}^{93}\text{Nb}$ reaction remains almost the same as we change the deformability parameter values from $\delta_1 = 6.6 \times 10^{-6}$ and $\delta_2 = 9.7 \times 10^{-9}$ (values calculated using rotating liquid drop model (RLDM) [19]), to $\delta_1 = 6.6 \times 10^{-4}$ and $\delta_2 = 9.7 \times 10^{-6}$. On the other hand, the α -particle spectra for the ${}^4\text{He} + {}^{58}\text{Ni}$ reaction showed significant change as we changed the deformability parameter from its RLDM values ($\delta_1 = 3.9 \times 10^{-5}$, and $\delta_2 = 4.5 \times 10^{-8}$). It was possible to fit the α -particle spectra in this case with higher values of the deformability parameters ($\delta_1 = 3.9 \times 10^{-4}$ and $\delta_2 = 5.5 \times 10^{-6}$). In fixing the δ values for the ${}^4\text{He} + {}^{58}\text{Ni}$ system we have taken the level density parameter as $a = A/9$; this has been fixed by fitting the neutron and the proton spectra, where

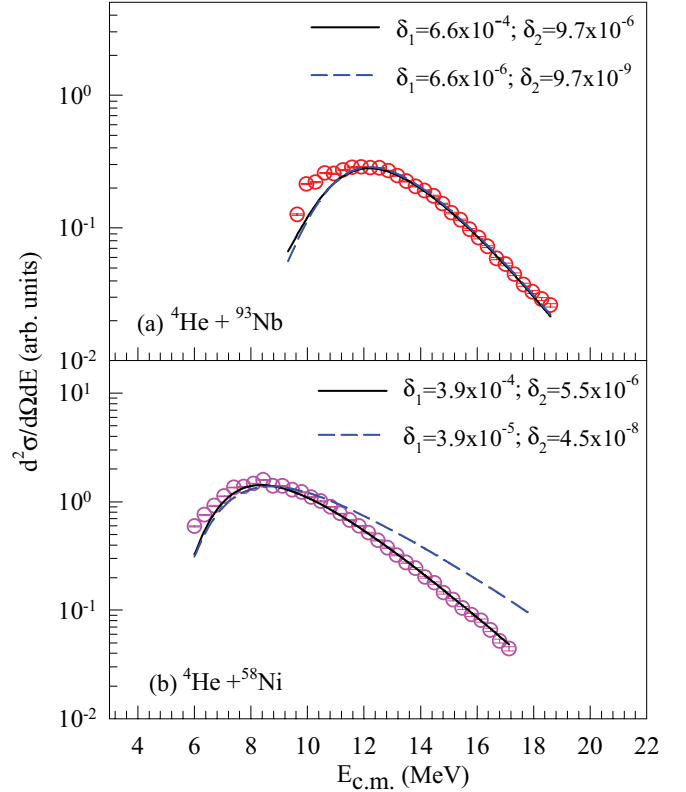


FIG. 5. (Color online) Effect of deformability parameters (δ_1, δ_2) in determining the shape of the α -particle spectra for (a) ${}^4\text{He} + {}^{93}\text{Nb}$ and (b) ${}^4\text{He} + {}^{58}\text{Ni}$ systems.

the spectra were only sensitive to a . For the ${}^4\text{He} + {}^{93}\text{Nb}$ system the RLDM values of δ_1 and δ_2 were used. For the analysis of the fold-gated spectra further variation of δ_1 and δ_2 could not explain the experimental data. Thus during the analysis of the particle spectra with different fold gating, all parameters other than the level density parameter were kept fixed to its ‘*all fold*’ value. The level density parameters were varied to get the best fit to the experimental data for different folds corresponding to different angular momentum region. The best fits to the experimental data were obtained by the chi-square minimization technique.

The best fit values of the inverse level density parameter as obtained from the theoretical fits to the neutron, proton, and α -particle energy spectra, for different folds, are given in Table I. The average angular momenta corresponding to different folds are also given in the table. It can be observed from Table I that the values of the inverse level density parameter decrease at higher folds (angular momentum) for both the systems. Although the absolute values of inverse level density parameter extracted from different particle spectra for the same fold are not exactly same, the decrease in k (or increase in a) at higher folds is observed from all three evaporation spectra consistently. The present observation on the angular momentum dependence of the level density parameter is in accordance with our earlier study of angular momentum gated neutron energy spectra in ${}^4\text{He} + {}^{115}\text{In}$ system [4]. The angular momentum dependence in NLD is generally taken care

TABLE I. Average angular momenta and inverse level density parameters for different γ folds.

System	Fold	$\langle J \rangle (\hbar)$	k from neutron	k from proton	k from α
$^4\text{He} + ^{93}\text{Nb}$	All	13.4 ± 4.3	9.9 ± 0.1	9.3 ± 0.3	10.7 ± 0.3
"	2	15.7 ± 5.7	9.7 ± 0.1	9.7 ± 0.8	10.4 ± 0.4
"	3	18.8 ± 5.9	9.5 ± 0.2	9.4 ± 1.1	8.4 ± 0.6
"	≥ 4	22.5 ± 6.7	8.2 ± 0.2	7.1 ± 1.4	6.0 ± 0.7
$^4\text{He} + ^{58}\text{Ni}$	All	11.6 ± 4.1	8.9 ± 0.4	9.0 ± 0.1	8.8 ± 0.4
"	2	13.5 ± 4.7	8.0 ± 0.5	9.3 ± 0.2	8.0 ± 0.5
"	3	15.8 ± 4.9	7.0 ± 0.7	8.8 ± 0.4	6.5 ± 0.5
"	≥ 4	18.8 ± 5.5	6.0 ± 0.8	8.2 ± 0.5	5.6 ± 0.7

through the rotational energy E_{rot} where the effect of angular momentum dependent deformation on the decay is introduced by the effective moment of inertia ($\mathfrak{I}_{\text{eff}}$). The deformability parameters (δ_1 and δ_2), which are generally adjusted to take care of the angular momentum dependent deformation, failed to reproduce the fold gated particle spectra. Although in the CASCADE calculations only the single particle level density [$\rho_{\text{int}}(E^*, J)$] is considered, the collective enhancement factors have also been estimated using the prescription of Ignatyuk *et al.*, [20] and Junghans *et al.*, [21]. The collective enhancement factors primarily depend on the value of quadrupole deformation parameter (β_2). For the present systems having quite small β_2 values, the calculated collective enhancement factors were found negligible. Moreover, as per the present formulations the collective enhancement factor does not depend on angular momentum explicitly, though there may be some weak dependence on angular momentum through the temperature. Therefore it is evident from the present analysis that the phenomenological NLD model [Eq. (1)] with RLDM prescription as well as consideration of collective enhancement factor [Eq. (4)] could not explain the general trend of the current data.

IV. SUMMARY AND CONCLUSIONS

The energy spectra of the evaporated neutrons, protons, and α particles in the reaction of ^4He on ^{93}Nb and ^{58}Ni have been measured at backward angles in coincidence with the γ rays of various multiplicities. The analysis of γ -ray fold-gated particle spectra have been carried out using the statistical model code CASCADE. From the present analysis it is observed that the value of k decreases with the increase of $\langle J \rangle$ for all three emissions, although there are some differences in the absolute values of the inverse level density parameter extracted from different particle spectra. The decrease of k at higher J is indicative of the fact that NLD increases with angular momentum. Shape change at higher angular momentum based on RLDM as well as the present prescription of collective enhancement failed to explain the observed variation of NLD with J . Microscopic calculations and further investigations will be useful in order to understand the observed phenomenon in more detail.

ACKNOWLEDGMENT

The authors are thankful to VECC Cyclotron operators for a smooth running of the accelerator during the experiment.

-
- [1] H. A. Bethe, *Phys. Rev.* **50**, 332 (1936); *Rev. Mod. Phys.* **9**, 69 (1937).
[2] S. Cohen, F. Plasil, and W. J. Swiatecki, *Ann. Phys. (NY)* **82**, 557 (1974).
[3] A. V. Ignatyuk, G. N. Smirenkin, and A. S. Tishin, *Sov. J. Nucl. Phys.* **21**, 255 (1975).
[4] K. Banerjee, S. Bhattacharya, C. Bhattacharya, M. Gohil, S. Kundu, T. K. Rana, G. Mukherjee, R. Pandey, P. Roy, H. Pai, A. Dey, T. K. Ghosh, J. K. Meena, S. Mukhopadhyay, D. Pandit, S. Pal, and S. R. Banerjee, *Phys. Rev. C* **85**, 064310 (2012).
[5] Y. K. Gupta, D. C. Biswas, Bency John, B. K. Nayak, A. Saxena, and R. K. Choudhury, *Phys. Rev. C* **80**, 054611 (2009).
[6] Y. K. Gupta, Bency John, D. C. Biswas, B. K. Nayak, A. Saxena, and R. K. Choudhury, *Phys. Rev. C* **78**, 054609 (2008).
[7] A. Mitra, D. R. Chakrabarty, V. M. Datar, Suresh Kumar, E. T. Mirgule, and H. H. Oza, *Nucl. Phys. A* **707**, 343 (2002).
[8] S. Björnholm, A. Bhor, and Mottelson, *Proceedings of the International Conference on the Physics and Chemistry of Fission, Rochester, New York, 1973* (IAEA, Vienna, 1974), Vol. 1, p. 367.
[9] R. J. Charity, *Phys. Rev. C* **82**, 014610 (2010).
[10] M. Aggarwal and S. Kailas, *Phys. Rev. C* **81**, 047302 (2010).
[11] K. Banerjee, T. K. Ghosh, S. Kundu, T. K. Rana, C. Bhattacharya, J. K. Meena, G. Mukherjee, P. Mali, D. Gupta, S. Mukhopadhyay, D. Pandit, S. R. Banerjee, S. Bhattacharya, T. Bandopadhyay, and S. Chatterjee *et al.*, *Nucl. Instrum. Methods Phys. Res. A* **608**, 440 (2009).
[12] Deepak Pandit, S. Mukhopadhyay, Srijit Bhattacharya, Surajit Pal, A. De, and S. R. Banerjee, *Nucl. Instrum. Methods Phys. Res. A* **624**, 148 (2010).
[13] G. Dietze and H. Klein, PTB-ND-22 Report, 1982.
[14] Deepak Pandit, S. Mukhopadhyay, Srijit Bhattacharya, Surajit Pal, A. De, and S. R. Banerjee, *Nucl. Instrum. Methods Phys. Res. A* **624**, 148 (2010).

- [15] F. Puhlhofer, *Nucl. Phys. A* **280**, 267 (1976).
- [16] D. Wilmore and P. E. Hodgson, *Nucl. Phys.* **55**, 673 (1964); P. E. Hodgson, *Annu. Rev. Nucl. Sci.* **17**, 1 (1967).
- [17] F. G. Perey, *Phys. Rev.* **131**, 745 (1963).
- [18] J. R. Huizenga and G. Igo, *Nucl. Phys.* **29**, 462 (1961).
- [19] A. J. Sierk, *Phys. Rev. C* **33**, 2039 (1986).
- [20] A. V. Ignatyuk, K. K. Istekov, and G. N. Smirenkin, *Sov. J. Nucl. Phys.* **29**, 450 (1979).
- [21] A. R. Junghans, M. de Jong, H. G. Clerc, A. V. Ignatyuk, G. A. Kudyaev, and K. H. Schmidt, *Nucl. Phys. A* **629**, 635 (1998).